Field Heterogeneity of Soil Organic Carbon and Relationships to Soil Properties and Terrain Attributes

D. R. Huggins and D. P. Uberuaga

USDA-ARS Land Management and Water Conservation Research Unit, Pullman, WA, 99164

david.huggins@usda.ars.gov, 509-335-3379 (work), 509-335-3842 (fax)

Abstract

Our objectives were to: (1) characterize SOC (0 to 1.53-m) within a 37-ha field typical of the Palouse region in eastern Washington; and (2) assess correlations and how much SOC variance could be accounted for by terrain and soil variables. A systematic, non-aligned grid of 177 geo-referenced sample locations was established at the Washington State University Cook Agronomy Farm (CAF) near Pullman, WA. Intact soil cores (0-153 cm) were collected, soils were described, classified, the surface divided into 0-30-cm increments and then by soil horizon to a depth of 153 cm and analyzed for soil bulk density and SOC. A digital elevation model (DEM) was developed and terrain attributes (slope, TRASP, curvature, global irradiation, flow accumulation and direction, specific catchment area, and wetness index) derived (10-m grid). Profile (0-153 cm) SOC ranged from 54 to 272 Mg C/ha over the 37-ha field and landscape SOC redistribution via soil erosion was evident. Terrain attributes and soil variables accounted for up to 86% of profile SOC variation; however, results were unique for each soil series. Redistribution of SOC via erosion increases field SOC heterogeneity and must be quantified if SOC sequestration and management impacts are to be adequately assessed.

Keywords: Soil organic C, terrain attributes, field variability

Introduction

Soil organic matter (SOM) has well-known critical functions in agricultural systems ranging from nutrient cycling and promotion of soil productivity (e.g. Seybold et al., 1997) to carbon sequestration and mitigation of global climate change (e.g. Lal, 2004). Despite its importance, quantifying SOM storage at the agricultural field scale is problematic, due in part to our lack of knowledge about field-scale processes and factors that regulate SOM dynamics. Field SOM heterogeneity occurs as a function of complex interactions of biological and physical processes (e.g. C inputs from crop residues and roots; SOM decomposition; soil erosion driven by water, wind and tillage translocation) (Gregorich et al., 1998; VandenBygaart et al., 2002; Huggins et al., 2007; Chaplot et al., 2009). In turn these processes are regulated by land use and management practices, soil properties, landscape attributes and climatic conditions that operate over time to develop site-unique SOM characteristics (Jenny, 1941). Greater understanding of field-scale variations of SOM and the processes and factors contributing to SOM dynamics is of key importance to quantifying soil organic C (SOC) sequestration, development of more sophisticated SOC models and for promoting improved land use and management decisions for precision conservation practices.

The Palouse region of eastern Washington and northern Idaho is the geological center of the loess deposit on the Columbia Plateau (McCool and Busacca, 1999). Distinctive soil-landscape patterns have formed in the loess deposits where Mollisols with topsoil thickness ranging from 0 (eroded knobs) to over one meter (pachic footslopes) are found within steeply sloping hills that have complex shapes (Busacca and Montgomery, 1992). Native SOC varied considerably within a given landscape ranging from about 2% on summit positions to almost 4.5% on north-facing footslopes (Rodman, 1988). Dryland agriculture has had a tremendous influence on native SOC primarily due to shifts from perennial bunch grass dominated vegetation (Daubenmire, 1970) to annual cropping, coupled with inversion tillage that has resulted in historical soil erosion rates of over 25 Mg soil yr^{-1} (USDA, 1978). Purakayastha et al. (2007) estimated that 50 to 70% of SOC had been lost from upland soils. Our objectives are to: (1) characterize SOC (0 to 1.53-m depth) within a 37-ha field with soil and terrain attributes typical of the Palouse region in Eastern Washington and Northern Idaho; and (2) assess correlations and how much SOC variance could be accounted for by terrain and soil variables.

Materials and Methods

A systematic, non-aligned grid of 369 geo-referenced sample locations was established in 1999 on 37 ha of the Washington State University Cook Agronomy Farm (CAF) near Pullman, WA. Previous history of the land included production of small grains (wheat and barley) using conventional inversion tillage practices. Intact soil cores (0-153 cm depth, 4.1 cm diameter) were collected at alternating points (177 cores) and profiles were described (Soil Survey Manual, 1993) to characterize soil horizon and morphological properties and to classify soil at the series level. Following classification, soil cores were divided by 10-cm increments to a depth of 30 cm and then by soil horizon to a depth of 153 cm for analyses of soil bulk density (subsample dried at 105^{o}C) and SOC (samples dried at 55^{o}C, ground to pass 2-mm sieve and soil C determined by dry combustion with a CNS Leco analyzer). Inorganic soil C was determined by a modified pressure-calcimeter method (Sherrod et al., 2002) and SOC for each sample was obtained by difference. SOC was expressed on a mass per unit area basis for depths of 0-30 cm, 30-153 cm and 0-153 cm using bulk density and soil C concentration data.

A digital elevation model (DEM) of the 37-ha field was developed using a survey grade differential global positioning system (DGPS; Trimble RTK 4400) comprised of a base station and a rover unit where elevation data with corresponding Easting and Northing values were collected in the fall of 1999. The projection used was Universal Transverse Mercator (UTM) with World Geodetic System (WGS) 1984 zone 11N datum. When operating with at least four satellites, the Trimble unit is capable of gathering measurements in the vertical and horizontal plane with an accuracy of 0.02 m every second (Trimble Navigation, 2001). A central location was selected for placement of the base unit so it could remain stationary for two hours to enable calculation of its position within 2 cm (Trimble Navigation, 2001) and to allow for continuous communication with the rover unit. The DGPS survey resulted in 30,440 Easting and Northing values with corresponding elevation data for the 37-ha field, an average of one point for every 12.16 m^2. The maximum predicted horizontal error was 2.74 cm with a mean of 1.09 cm, while the maximum predicted vertical error was 4.56 cm with a mean of 1.74 cm.

A series of increasing raster cell size DEMs, 1-m, 2-m, 5-m, 10-m, 15-m, 20-m, 25-m, and 30-m, were created using a Local Polynomial Interpolation (LPI) with 30% global and 70% local polynomial influence (ESRI ArcGIS v. 8.2). Terrain attributes derived from the resulting DEMs were slope (degrees), plan curvature (radians $100m^{-1}$), profile curvature (radians $100m^{-1}$), tangential curvature (radians $100m^{-1}$), flow accumulation (no. of x-m^2 cells, where x is the raster cell size), flow direction, specific catchment area (m), wetness index and aspect (ESRI ArcGIS v. 8.2). Aspect was transformed to TRASP = (1-cos((π/180)(aspect-30)))/2. Global solar irradiation (MegaWatt Hours m^{-2} yr^{-1}) was calculated using Solar Analyst Extension for ArcView 3.0 (HemiSoft Inc) based on a combination of direct and diffuse solar irradiation. The 177 geo-referenced soil sample data points were combined with the terrain attributes calculated from the 10-m raster for subsequent statistical analyses.

A kinematic survey of apparent electrical conductivity (EC_a) was conducted using an EM38 (Geonics Limited, 2000) operated in the vertical dipole mode and coupled with a Trimble Ag 132 Differential GPS (DGPS), UTM WGS84 zone 11N. When operated in the vertical dipole mode, the effective measurement depth is about 1.5 m (Sudduth et al., 2001). Readings from the EM38 were coupled with location data provided by the DGPS every second using the HGIS (StarPal 1997) software package. The EC_a survey was conducted twice: March 25, 2000, just prior to planting spring barley (*Hordeum vulgare* L.), and on September 14, 2000, following spring barley harvest. The output text files were imported into Geostatistical Software Library (GSLIB, Deutsch and Journel, 1992) where interpolation of both the spring and fall EC_a data was accomplished using ordinary kriging.

Crop yields of wheat (*Triticum aestivum* L.), barley, peas (*Pisum arvense* L.) and canola (*Brassica napus annua* Koch) were sampled at each of the 369 geo-referenced points (2-m^2 sample area) for five years (1999-2003) to determine relative yield (crop yield at each point divided by the largest crop yield) each year and to calculate the average relative yield for each geo-referenced point. Relative yield data were interpolated using ordinary kriging (GSLIB, Deutsch and Journel, 1998) to display field spatial patterns.

Soil organic C data were spatially mapped using inverse distance square interpolation. Analyses of SOC using ordinary kriging and co-kriging did not yield maps with satisfactory error terms and were not used to display spatial patterns. Statistical analyses of terrain attributes, ECa, soil and yield data were based on values from the 177 geo-referenced locations. Analysis of variance was used to assess soil series (USDA-SCS, 1980) and field soil map unit (field soil description and classification) differences in SOC for depth-increments of 0-30 cm, 30-153 cm and 0-153 cm (Proc Mixed, SAS, v. 9.1.3). Pearson correlation coefficients ($p \leq 0.05$) were determined by soil map unit among SOC, soil descriptive properties, relative crop yield and terrain attributes. Multiple regression models were developed using stepwise selection of explanatory variables ($p \leq 0.15$) by soil map unit to assess partial and model R^2 of variables related to SOC (Proc Reg, SAS, v. 9.1.3). Models were tested for lack of multicollinearity, equal error variance (no heteroscedasticity) and normal and random residuals (Neter et al., 1990). Mallows C(p) was used to prevent over-parameterization of regression models. Our goal was to examine models for the field of study rather than to extrapolate their use for SOC prediction on similar soils and landscapes of the region.

Results

Soil Organic Carbon and Soil Map Units

Soil profile (0-153 cm) SOC ranged from 54 to 272 Mg C ha^{-1} and averaged 131 Mg C ha^{-1} over the 37-ha field (Figure 14.1, Table 14.1).[1] The largest SOC contents were found in northern aspects and bottomlands where moderately well-drained Thatuna silt loams predominate with inclusions of somewhat poorly drained Latah and Caldwell series soil (Figure 14.1). Soil survey mapped Thatuna silt loams averaged 149 Mg C ha^{-1} followed by Palouse (125 Mg C ha^{-1}) and Naff (111 Mg C ha^{-1}) series soil (Table 14.1). The smallest SOC profile contents were associated with southern aspects and upland ridge-top and knob positions, particularly well-drained Staley silt loams (profile SOC averaging 97 Mg C ha^{-1}), which were found as inclusions among soil survey areas of upland, well-drained, Palouse and Naff silt loams (Figure 14.1, Table 14.1).

The SOC in the surface 30-cm ranged from 26 to 79 Mg C ha^{-1} (mean of 56 Mg C ha^{-1}) and was positively related in many, but not all, locations to subsoil (30-153 cm) SOC (Figure 14.2). Subsoil SOC (30-153 cm) averaged 75 Mg C ha^{-1} (range of 14-193 Mg C ha^{-1}) and had CV's of up to 2.3 times greater than surface SOC within a given soil map unit (Table 14.1). The ratio of surface to subsurface SOC averaged 0.83 and ranged from 0.33 to 3.93 (Figure 14.2).

Descriptions of the 177 soil cores revealed inclusions of Staley, Latah and Caldwell series soil within the field (Figure 14.1, Table 14.1). The SOC in Staley silt loams was significantly less ($p \leq 0.05$) than that found in other soils while both Latah and Caldwell silt loams were not significantly different than SOC in Thatuna series soil and occupy similar landscape positions (Table 14.1). Consequently, Staley, Naff, Palouse and Thatuna series soil were used in subsequent analyses where the data from Latah and Caldwell series soil were combined with data from Thatuna silt loams.

Soil Properties, Crop Yield and Soil Organic Carbon

The thickness of the A horizon was positively correlated to surface, subsurface and profile SOC in Naff, Palouse and Thatuna series soil (Table 14.2). In contrast, however, A horizon thickness was only related to subsoil SOC in Staley series soil (Table 14.2). Lack of correlation of surface SOC to A horizon thickness in Staley series soil occurred as A horizon thickness averaged 36 cm and was often limited to a depth defined by inversion plowing (Ap horizon) with a distinct boundary occurring between the Ap and a Bk horizon below. The SOC concentrations were lower in Staley silt loams as compared to all other soils (data not shown) evidence that the combination of soil erosion and mixing of A and B horizon materials by tillage has likely diluted A horizon SOC over time. Subsoil SOC was positively influenced at locations where the A horizon of Staley series soil extended past 30 cm, an indication that soil erosion had not completely removed the original A horizon.

The depth to the top of a B horizon (e.g. Bw, Bt, Bk) was positively correlated to SOC in many instances, but was highly dependent on soil map unit (Table 14.2). Whereas Bw horizons occurred within all soil map units and were often the only B horizon found within Palouse soils, Bk horizons were restricted to Staley series soil and Bt horizons were primarily found in Naff

[1] Because of their size, all figures and tables for this chapter are at the end.

and Thatuna silt loams. The greatest correlation coefficients (0.75 and 0.85 for subsoil and profile SOC, respectively) occurred between depth of the Bk horizon and the SOC in Staley series soil. Depth of the Bw horizon was positively correlated with SOC in Naff and Palouse series soil, while Bt depth was significant in Thatuna series soil. High positive correlations also occurred between the depth of E horizons in Thatuna series soil and SOC in the subsurface and total profile. Not surprisingly, all of the B and E horizon depths were positively correlated with A horizon thickness (data not shown).

Apparent soil electrical conductivity measured in the spring (EC_aS) was negatively correlated to topsoil SOC (0-30 cm) in Naff, Palouse and Thatuna silt loams. The only correlation of EC_aS with subsoil and profile SOC occurred in Thatuna series soil. Positive correlations were found between soil EC_a and the presence of a Bt or E horizon, while negative correlations were found between EC_a and Bt and E horizon depth (data not shown). Soil EC_a is sensitive to fluctuations in electrical conductivity due to soil salinity, clay content, soil water content, cation exchange capacity and temperature (McNeill, 1992; Suddeth et al. 1997; Mueller et al., 2003; Shaw and Mask, 2003). The negative correlations of EC_a measured in the spring and fall to SOC are likely indirect consequences of the positive correlation found between EC_a and subsoil clay found in Bt horizons (data not shown). Here, increasing EC_a is related to erosion processes as clay enriched Bt horizons are gradually exposed with the erosion of topsoil from Naff and Thatuna series soil.

Average relative crop yield (Ryld) across five years ranged from 0.38 to 0.80 and was positively correlated with surface SOC in Naff, Palouse and Thatuna series soil and the subsoil SOC of Staley series soil (Table 14.2). The positive correlation of 0.87 found between subsoil SOC of Staley series soil and relative yield was the largest correlation of any measured variable with SOC.

Stepwise regression showed that soil variables explained a substantial amount of study area SOC variability in some cases. The largest regression model R^2 for SOC, using only soil variables, were topsoil SOC in Naff series soils (R^2 = 0.58), and subsoil SOC for Staley (R^2 = 0.64) and Thatuna (R^2 = 0.57) series soil (Table 14.3). In the Staley and Thatuna series soil, regression models for subsoil SOC contained Bk and E depth, respectively, as the only significant model variables. Surface SOC variability in both of these soils was poorly explained by regression models comprised of the soil variables measured. A horizon thickness was the most important soil property explaining the variation in SOC regression models of Naff and Palouse series soil (Table 14.3). Overall, regression analyses of soil profile SOC had similar R^2 for Staley (0.47), Palouse (0.49) and Thatuna (0.48) series soil while the model R^2 for Naff series soil was lower (0.40) (Table 14.3).

Adding relative yield to soil variables in Table 14.3 significantly increased the amount of SOC variability explained by regression models for Staley series topsoil, subsoil and profile SOC (R^2 increased to 0.18, 0.84 and 0.70, respectively). No increase in regression R^2 occurred, however, when relative yield was added to model variables for subsoil and profile SOC of Naff, Palouse and Thatuna series soil. Here, only topsoil SOC model R^2 increased for Naff (R^2 = 0.63), Palouse (R^2 = 0.40) and Thatuna (R^2 = 0.19) series soil.

Terrain Attributes and Soil Organic Carbon

Elevation and derived terrain attributes varied widely across the study area (Figure 14.3). Elevation ranged from 773 to 814 m and was positively correlated to the SOC of Thatuna series surface soil (0-30 cm) (Table 14.4). Slope ranged from 0 to 18.6 degrees in the 37-ha field (Figure 14.3) and was negatively correlated (-0.61) with Naff series surface SOC (Table 14.4). Slope was the only terrain attribute related to SOC in Naff series soil. In contrast, slope was positively correlated with Palouse and Thatuna series subsoil and soil profile SOC and Thatuna series surface SOC (Table 14.4).

Global irradiation (GloIrr) is the sum of direct and diffuse global irradiation cumulated over a year (MegaWatt-hours m^{-2} yr^{-1}). GloIrr on the CAF ranged from about 1.2 to 1.9 MegaWatt-hours m^{-2} yr^{-1} and is primarily a function of aspect and slope (Figure 14.3). Transformation of aspect to TRASP resulted in values that ranged from zero for land oriented in a north-northeast direction, (typically the coolest and wettest orientation) to a value of one for south-southwesterly slopes that are usually the hottest and driest. Both GloIrr and TRASP were negatively correlated with subsoil and profile SOC of Staley series soils while GloIrr was also negatively correlated with subsoil and profile SOC of Palouse series soil.

Plan curvature is in the horizontal plane of a contour line, profile curvature is in the vertical plane and tangential curvature is in an inclined plane perpendicular to both the direction of flow and the surface (Figure 14.3). Convex curvatures are positive while concave curvatures are negative values. Values of tangential curvature ranged from -0.26 to 0.24 radians $100m^{-2}$ and the field patterns for the CAF looked nearly identical to plan curvature in Figure 14.3 and therefore were not displayed. Tangential and plan curvature were negatively correlated (to -0.50) with all Palouse series SOC values while profile curvature was positively correlated (to 0.59) with Palouse series SOC (Table 14.4). Tangential and plan curvature were also negatively correlated with Staley subsoil SOC (-0.64 and -0.55, respectively) and plan curvature negatively correlated with profile SOC (-0.55) in Staley series soil. In addition, profile curvature was positively correlated with subsoil SOC (0.30) of Thatuna series soil.

Flow direction (FlowD) is the primary direction of surface water flow and an approximate surrogate for aspect, in this case representing eight compass directions (Figure 14.3). Flow direction was highly correlation with Staley series surface, subsoil and profile SOC with coefficients of 0.57, 0.65 and 0.72, respectively. However, FlowD was not significantly correlated with SOC of any other soil series (Table 14.4). Flow accumulation (FlowA) is the amount of accumulated area along a flow direction (FlowD) and for the CAF, FlowA ranged from 0 to 11775 cells of five m^2 each (Figure 14.3). Flow accumulation was positively correlated with profile SOC of Palouse series soil and negatively correlated with the surface SOC of Thatuna series soil.

Specific catchment area (SCA) is the upslope contributing area (the area above a defined length of contour that contributes flow across the contour) divided by the contour length. The contour length is approximately the size of a grid cell and the contributing area is determined by the number of grid cells contributing flow to a downslope cell. Therefore, the SCA is equal to FlowA/grid cell size and map patterns were identical to FlowA (Figure 14.3) and not displayed. Wetness index (WetInd) or compound topographic index is a quantification of catenary landscape position that integrates SCA and slope angle: $WetInd = \ln(SCA/\tan\beta)$ where SCA is previously defined and β is the slope angle (Gessler et al. 2000). The WetInd ranged from 0 to 16.7 for the CAF with upland landscape positions having smaller values than lower landscape positions (Figure 14.3). Both SCA and WetInd were positively correlated with SOC of Palouse series soil while SCA was negatively correlated with the surface SOC of Thatuna series soil.

Stepwise regression showed that terrain variables explained from 0 to 75% of the variance in SOC (Table 14.5). The largest amount of SOC variability explained by terrain attributes occurred in Staley series soil where FlowD and in some cases plan and tangential curvature, GloIrr and elevation contributed to model R^2 of 0.47, 0.75 and 0.73 for surface, subsurface and profile SOC, respectively. In Naff series soil, relatively high amounts of variation in surface SOC were explained by slope, plan and tangential curvature and elevation (R^2 = 0.54); however, little variation in subsurface and total profile SOC was explained by terrain attributes. In contrast to Naff series soil, Palouse series subsoil and total SOC had the largest regression model R^2 while variation in surface SOC was poorly explained by terrain variables. The largest contribution toward accounting for Palouse series subsoil and profile SOC variability was profile curvature (partial R^2 = 0.35 and 0.32, respectively). Relatively moderate success was achieved in explaining Thatuna series SOC variability with terrain attributes (R^2 = 0.33, 0.22 and 0.25 for surface, subsurface and profile SOC, respectively). Slope and profile curvature were consistent contributors to model R^2, with SCA, FlowA, plan curvature, GloIrr and elevation also contributing toward explaining variations in Thatuna series SOC in some cases (Table 14.4).

Soil Properties, Terrain Attributes, Relative Yield and Soil Organic Carbon

The combination of soil and terrain variables provided regression models that explained the largest amount of SOC variability with model R^2 ranging from 0.32 to 0.87 (Table 14.6). Only regression models of Staley series surface SOC and Naff series subsoil and profile SOC failed to improve by including both soil and terrain variables. No consistent set of soil and terrain variables explained variations in SOC across all soil mapping units (Table 14.6). Ranking of regression model effectiveness in explaining surface SOC was Naff series (R^2 = 0.66), Thatuna series (R^2 = 0.48), Staley series (R^2 = 0.48) and Palouse series (R^2 = 0.32). This ranking almost completely reversed for explaining subsoil SOC: Staley series (R^2 = 0.85), Palouse series (R^2 = 0.77), Thatuna series (R^2 = 0.59) and Naff series (R^2 = 0.34).

Including relative yield as an explanatory variable along with soil and terrain variables increased regression model R^2 for surface SOC of Palouse (R^2 = 0.44) and Thatuna (R^2 = 0.53) , but not for Staley or Naff (data not shown). The only other cases where including relative yield improved regression model R^2 were for Staley subsurface SOC (R^2 = 0.96) and profile SOC (R^2 = 0.94), the highest R^2 values found in the study.

Discussion

The five-fold range in soil profile SOC (0-1.53 m) illustrates the tremendous within-field variability of SOC that has typically been found in the Palouse region (Figure 14.1; Rodman, 1988; Busacca and Montgomery, 1992). The SOC variability was expressed within all soil map units and neither soil survey nor more detailed field map units explained much of this heterogeneity (Table 14.1, Figures 14.1 and 14.2). Field SOC was usually greater and more variable in the subsoil (30-153) than in surface (0-30 cm) soil (Table 14.1; Figure 14.2). Consequently, these data strongly support the necessity of soil sampling beyond surface depths if

SOC sequestration is to be adequately assessed as suggested by Baker et al., 2007 and concluded by Blanco-Canqui and Lal, 2008. Process-oriented modeling to predict management effects on field-scale SOC will also be challenged by this extreme variability as initial SOC levels will be required to initiate models and will also impact subsequent changes in SOC due to shifts in agricultural management (Ismail et al. 1994; VandenBygaart, 2002). Furthermore, the development of precision conservation strategies that tailor management practices to site-specific conditions will require knowledge of within-field SOC variability. For example, locations of Conservation Reserve Program plantings or other conservation-based practices might target field areas with low SOC, while precision nutrient management will require knowledge of SOM cycling and the bioavailability of N, P, S and other essential nutrients associated with different within-field levels of SOC or as affected by decreased SOM buffering and adverse subsoil properties (Pan and Hopkins, 1991; Pan et al., 1992; Fiez et al., 1995).

Although considerable landscape level variability in native SOC was present before the advent of dryland farming (Busacca and Montgomery, 1992) it is likely that soil erosion processes, accelerated by the onset of dryland farming practices have increased SOC variability. In the Palouse region of eastern Washington, soil erosion due to agricultural practices has been estimated to have removed 100% of the topsoil from 10% of the landscape with another 25 to 75% loss from 60% of agricultural land (USDA, 1978). Not often recognized or measured, however, is the effect of soil erosion processes on within-field soil deposition and likely site-specific increases in SOC stocks.

Soil erosion processes of particle detachment, sediment transport and deposition either within fields or associated surface waters are receiving increased scrutiny as important factors influencing field-scale SOC budgets (De Jong and Kachanoski, 1988; Starr et al., 1999; Fang et al., 2006; Chaplot et al., 2009). Soil erosion is a selective process and transported sediments are enriched in clay-sized particles (Ongley et al., 1981) as well as particulate and dissolved organic C (Lal, 1995). In this study, the large ratios of surface to subsurface SOC are indicative of field areas where soil erosion processes of detatchment and transport have been more dominant than soil deposition, resulting in net SOC losses and redistribution to downslope field locations or transport out of the field (Figure 14.2). In contrast, low surface to subsurface SOC ratios indicate areas where deposition of SOC has occurred and/or areas where transported subsoil from historically eroded upland areas with low SOC concentrations, have buried the previous topsoil. The close proximity of areas with low and high surface to subsoil SOC ratios indicates a coupling of soil detachment, transport and deposition within the field that has likely contributed to the large within-field variability of SOC stocks (Figure 14.2, Table 14.1). Furthermore, scouring of soil from field areas susceptible to concentrated water flow and the formation of surface gullies followed by subsequent deposition of soil with low SOC concentrations could explain the occurrence of low SOC stocks and surface to subsoil SOC ratios in footslope positions (Figure 14.2).

Erosion-related processes that laterally redistribute SOC, thereby removing and/or depositing SOC from different field locations, can be as important as inputs and losses of SOC due to biological processes for determining SOC stocks at a specific site. In fact, historical soil erosion processes have likely decoupled current SOC stocks from the common expectation that SOC will be linearly related to C inputs (Larson et al., 1972; Rasmussen and Collins, 1991; Huggins et al., 1998). This raises the question as to whether or not current C inputs and decomposition regimes are capable of maintaining the SOC in areas with disproportionately large SOC stocks if soil erosion is curtailed. This will be somewhat dependent on the mean residence time of the buried, subsoil SOC and is a good area for future research. Redistribution of SOC due to erosion processes also has important implications for methods used to assess changes in SOC due to management practice. Whereas the importance of sampling to soil depths that extend beyond the surface has recently been emphasized for evaluating changes in SOC that occur when shifting from conventional inversion tillage (CT) to no-tillage (NT) (Huggins et al., 2007; Baker et al., 2007; Blanco-Canqui and Lal, 2008), collecting spatial data across representative landscapes is likely equally important if soil erosion processes have been operative. Across the field border comparisons of SOC under CT *versus* NT could conceivably show increases, decreases or little change in SOC depending on the soil erosion history and landscape position sampled. Furthermore, if baseline sampling is conducted and a change in management imposed that impacts soil erosion processes, either positively or negatively, sampling of representative landscapes would still be critical to the assessment of treatment effects on SOC as reported by VandenBygaart et al. (2002).

Several soil properties were important for explaining field-scale SOC variability (Table 14.2 and 14.3). Not surprisingly, A horizon thickness (the mollic epipedon) was often positively correlated with SOC levels (Table 14.2) as A horizons are zones of biological activity and SOM accumulation. In the Palouse region, the thickness of the A horizon is a function of original loess deposition, subsequent pedogenesis and soil erosion history. For example, in field locations where relatively young loess deposits were naturally thin such as summit positions, steep south slopes and convex midslope knobs, (Busacca and Montgomery, 1992; McCool and Busacca, 1999), A horizons of native soil were relatively thin and were highly susceptible to degradation by agricultural practices that accelerated erosion. The fact that A horizon thickness was not correlated with the surface SOC of the Staley series soil, which is found in upland, often convex landscape positions, illustrates the vulnerability of these soils to SOC decline via soil erosion. Soil properties differ across fields in the Palouse not only from the thickness of recent loess deposits, but also due to properties of older loess deposits that lie beneath younger loess (Busacca et al., 1985). The older loess contains paleosols that are often more dense, less permeable and less productive than soils formed in recent loess as these soils have, in higher precipitation zones, accumulations of clay (argillic horizons). Naff and Thatuna series soil typically have restrictive paleosol horizons (eg. Bt and E horizons) that limit water storage and root exploration and, as soil erosion diminishes topsoil depth, are increasingly unfavorable to biomass production (Bramble-Brodahl et al., 1985; Busacca et al., 1985; Hopkins and Pan, 1991). On the other hand, erosion processes that transport SOC enriched material to lower landscape positions could result in deeper Bt and E horizon surfaces and could favor biomass production as well as SOC accumulation in these field locations. Overall, the presence of Bt or E horizons within the sampled depths (0-1.53 m) along with depth to their surface was often correlated to SOC in Naff and Thatuna series soil and aided explanation of SOC variability (Tables 14.2 and 14.3).

Topography and terrain attributes are increasingly being utilized to provide insights into explaining field-scale SOC variability (Moore et al., 1993; Gessler et al., 2000; Bergstrom et al., 2001; Mueller and Pierce, 2003; Terra et al., 2004; Senthilkumar et al., 2009). Ritchie et al., (2007) reported negative correlations of SOC with slope gradient increases and greater accumulation of SOC on concave than on convex slopes. Terra et al., (2004) found that elevation, slope and compound topographic index (equivalent to wetness index) along with silt content and ECa explained up to 50% of the SOC variability. Our results support these findings as we could account for up to 75% of SOC variability using easily derived terrain attributes (Table 14.5). Notably, the contribution of different terrain attributes was specific for each soil series and likely reflects the landscape setting of the soil. Nevertheless, curvature, either plan, tangential or profile often contributed across all soil types to the explanation of SOC variability (Tables 14.4 and 14.5). Concave plan and tangential curvature represent convergent landscape positions that would promote soil deposition and the accumulation of SOC, while convex plan and tangential curvature represent divergent landscape positions where losses of water and sediment would be enhanced (Gessler et al., 2000). Negative correlations of plan and tangential curvature with SOC occurred in both Staley and Palouse series soil (Table 14.4) indicating that as convex curvature increased, SOC decreased. In contrast, positive correlations of profile curvature with SOC were found in Palouse and Thatuna series soil (Table 14.4). Here, convex slopes could be a barrier to the downslope movement of water and sediment thereby increasing deposition and the accumulation of SOC, while concave profile curvature could accelerate erosion processes. Flow accumulation, specific catchment area and wetness index were also important variables that were positively correlated with SOC, but only in Palouse series soil (Table 14.4) suggesting that soil erosion has contributed to SOC accumulation in lower landscape positions of this soil. Overall, terrain attributes accounted for 73% of profile SOC variability of Staley series soil and this relatively high model R^2 is likely a function of erosion processes where upland, convex slope positions have contributed to transportation of soil away from the site, but have little opportunity to receive soil deposition. This contrasts to other soil series that are found across more diverse landscape positions where erosion processes can lead to both transport and deposition of soil and SOC.

Summary and Conclusions

Our results show that SOC varies tremendously over short distances in this 37-ha field and that subsoil SOC (30 to153 cm) is more variable and, on average, contains greater SOC stocks than surface SOC (0 to 30 cm). The processes regulating field-scale SOC variability are complex, but relate strongly to terrain attributes and soil properties. In particular, the cumulative effects of soil erosion processes and the within-field transport and deposition of SOC have been major contributors to SOC variability. We could account for up to 86% of profile SOC variability (Staley series soil) when using a combination of terrain attributes and soil descriptive information. For Naff series soil, however, we could account for only 40% of profile SOC variability. This result could be a function of greater complexity in erosion processes of soil transport and deposition that impacts SOC storage. More research is needed to understand not only the effects of landscape processes on SOC redistribution, but the effects of this redistribution on site-specific SOC dynamics; for example, the dynamics of SOC in depositional areas where large stocks of SOC have accumulated. Soil sampling methodology and simulation modeling of SOC will need to incorporate landscape processes and effects that result in SOC redistribution if within-field stocks of SOC are to be quantified and in order to fully assess the impact of management changes on SOC, particularly when erosion processes are operative. The large within-field variability in SOC should be considered in the application of precision conservation practices such as site-specific nutrient management and placement of vegetative buffers and conservation plantings.

References

Baker, J.M., T.E. Ochsner, R.T. Venterea, and T.J. Griffi s. 2007. Tillage and soil carbon sequestration: What do we really know? Agric. Ecosyst. Environ. 118:1–5.

Bell, J.C., C.A. Butler, and J.A. Thompson. 1995. Soil-terrain modeling for site-specific agricultural management. p. 209-228. *In* P.C. Robert et al., (ed.) Site-specific management for agricultural systems. ASA Misc. Publ., ASA, CSSA, and SSSA, Madison, WI.

Bergstrom, D.W., C.M. Monreal, and E. St. Jacques. 2001. Spatial dependence of soil organic carbon mass and its relationship to soil series and topography. Can. J. Soil Sci. 81:53-62.

Blanco-Canqui and R. Lal, 2008. No-Tillage and Soil-Profile Carbon Sequestration: An On-Farm Assessment. Soil Sci. Soc. Am. J. 72:693-701.

Bramble-Brodahl, M., M.A. Fosberg, D.J. Walker, and A.L. Falen. 1985. Changes in soil productivity related to topsoil depth on two Idaho Palouse soils. pp. 18-27. *In:* Erosion and Soil Productivity, Proceedings of the National symposium on Erosion and Soil Productivity, New Orleans, 10-11 December, 1984. American Society of Agricultural Engineers, St. Joseph, MI.

Busacca, A.J., D.K. McCool, R.I. Papendick, and D.L. Young. 1985. Dynamic impacts of erosion processes on productivity of soils in the Palouse. pp. 152-169. *In:* Erosion and Soil Productivity, Proceedings of the National symposium on Erosion and Soil Productivity, New Orleans, 10-11 December, 1984. American Society of Agricultural Engineers, St. Joseph, MI.

Busacca, A.J., and J.A. Montgomery. 1992. Field-landscape variation in soil physical properties of the Northwest dryland crop production region. In Veseth, R. and B. Miller (ed.), Precision Farming for Profit and Conservation. 10th Inland Northwest Conservation Farming Conference Proceedings, Washington State University, Pullman.

Chaplot, V., P. Podwojewski, K. Phachomphon, C. Valentin. 2009. Soil erosion impact on soil organic carbon spatial variability on steep tropical slopes. Soil Sci. Soc. Am. J. 73:769-779.

De Jong, E., R.G. Kachanoski. 1988. The importance of erosion in the carbon balance of prairie soils. Canadian Journal of Soil Science 68:111-119.

Deutsch, C.V. and A.G. Journel. 1998. GSLIB Geostatistical Software Library and User's Guide. Second edition. Oxford University Press, New York, NY. 369 pp.

Fang, H.J., S.L. Cheng, X.P. Zhang, A.Z. Liang, X.M. Yang and C.F. Drury. 2006. Impact of soil redistribution in a sloping landscape on carbon sequestration in northeast China. Land Degrad. Develop. 17:89-96.

Fiez, T. E., W. L. Pan, and B. C. Miller. 1995. Nitrogen efficiency analysis of winter wheat among landscape positions. Soil Sci. Soc. Am. J. 59:1666-1671.

Gessler, P.E., I.D. Moore, N.J. McKenzie, and P.J. Ryan. 1995. Soil-landscape modelling and spatial prediction of soil attributes. Int. J. Geographical Information Systems 9(4):421–432.

Gessler, P.E., O.A. Chadwick, F. Chamran, L.D. Althouse, and K. Holmes. 2000. Modeling soil-landscape and ecosystem properties using terrain attributes. Soil Sci. Soc. Am. J. 64:2046–2056.

Gregorich, E.G., K.J. Geer, D.W. Anderson, and B.C. Liang. 1998. Carbon distribution and losses: Erosion and deposition effects. Soil Tillage Res. 47:291–302.

Huggins, D.R., G.A. Buyanovsky, G.H. Wagner, J.R. Brown, R.G., Darmody, T.R. Peck, G.W. Lesoing, M.B. Vanotti, and L.G. Bundy. 1998. Soil organic C in the tallgrass prairie−derived region of the corn belt: effects of long-term crop management. Soil Tillage Res. 47:219−234.

Huggins, D.R., R.R. Allmaras, C.E. Clapp, J.A. Lamb, and G.W. Randall. 2007. Corn-Soybean Sequence and Tillage Effects on Soil Carbon Dynamics and Storage. Soil Sci. Soc. Am. J. 71: 145-154.

Ismail, I., R.L. Blevins, and W.W. Frye. 1994. Long−term no tillage effects on soil properties and continuous corn yields. Soil Sci. Soc. Am. J. 58:193−198.

Jenny, H. 1941. Factors of soil formation: a system of quantitative pedology. McGraw-Hill Book Company, Inc., New York, NY.

Lal, R. 1995. Global soil erosion by water and carbon dynamics. pp. 131-142. *In:*R. Lal, J.M. Kimble, R.F. Follett and B.A. Stewart (eds.) Management of Carbon Sequestration in Soil. CRC Press, Boca Raton, FL.

Lal, R., 2004. Soil carbon sequestration impacts on global climate change and food security. Science 304, 1623-1627.

Larson, W.E., C.E. Clapp, W.H. Pierre, and Y.B. Morachan. 1972. Effect of increasing amounts of organic residues on continuous corn: II. Organic carbon, nitrogen, phosphorus, and sulfur. Agron. J. 64:204-208.

McCool, D.K. and A.J. Busacca. 1999. Measuring and modeling soil erosion and erosion damages. pp. 23-56 *In:*E.L. Michalson, R.I. Papendick and J.E. Carlson (eds.) Conservation farming in the United States: the methods and accomplishments of the STEEP program. CRC Press, Boca Raton, FL.

McNeill, J.D. 1992. Rapid, accurate mapping of soil salinity by electromagnetic ground conductivity meters. Advances in Measurement of Soil Physical Properties: Bringing Theory Into Practice. Spec. Publ. 20, SSSA, Madison, WI, 209-229.

Moore, I.D., P.E. Gessler, G.A. Nielsen, and G.A. Peterson. 1993. Soil attribute prediction using terrain analysis. Soil Sci. Soc. Am. J. 57:443–452.

Mueller, T.G., N.J. Hartsock, T.S. Strombaugh, S.A. Shearer, P.L. Cornelius, and R.I. Barnhisel. 2003. Soil electrical conductivity map variability in limestone soils overlain by loess. Agron. J. 95:496-507.

Mueller, T.G. and F.J. Pierce. 2003. Soil carbon maps: enhancing spatial estimates with simple terrain attributes at multiple scales. Soil Sci. Soc. Am. J. 67:258-267.

Neter, J.W., Wasserman, and M.H. Kutner. 1990. Applied linear regression models. Third edition. IRWAN. Homewood, IL. 1181 pp.

Ongley, E.D., M.C. Bynoe, and J.B. Percival. 1981. Physical and geochemical characteristics of suspended solids, Wilton Creek, Ontario. Canadian Journal of Earth Sci. 18:1365-1379.

Pan, W.L., T. Fiez, B. Miller, and A. Kennedy. 1992. Variable soil biological and chemical factors to consider in landscape management. *In:*R. Veseth and B. Miller (eds.) Precision Farming for Profit and Conservation, 10th Inland Northwest Conservation Farmng Conference Proceedings, Washington State University, Pullman, 20-25.

Pan, W.L., and A.G. Hopkins. 1991. Plant development, and N and P use of winter barley. I. Evidence of water stress-induced P deficiency in an eroded toposequence. Plant Soil 135:9-19.

Purakayastha, T.J., D.R. Huggins, J.L. Smith. 2008. Carbon sequestration in native prairie, perennial grass, no-till, and cultivated Palouse silt loam. Soil Sci. Soc. Am. J, 72(2): 534-540.

Paustian, K., W.J. Parton, and J. Persson. 1992. Modeling soil organic matter in organic-amended and nitrogen-fertilized long-term plots. Soil Sci. Soc. Am. J. 56:476-488.

Rasmussen, P.E., and H.P. Collins. 1991. Long-term impacts of tillage, fertilizer, and crop residue on soil organic matter in temperate semi-arid regions. Adv. Agron. 45:93-134.

Ritchie, J.C., G.W. McCarty, E.R. Venteris and T.C. Kasper. 2007. Soil and soil organic carbon redistribution on the landscape. Geomorphology 89:163-171.

Rodman, A.W., 1988. The effect of slope position, aspect, and cultivation on organic carbon distribution in the Palouse, Master's thesis. Washington State University, Pullman, 164 pp.

SAS Institute Inc. 2009. SAS OnlineDoc® 9.2. Cary, NC: SAS Institute Inc.

Senthilkumar, S., A.N. Kravchenko, and G.P. Robertson. 2009. Topography influences management system effects on total soil carbon and nitrogen. Soil Sci. Soc. Am. J. 73:2059-2067.

Seybold, C.A., M.J. Mausbach, D.L. Karlen, and H.H. Rogers. 1997. Quantification of soil quality. P. 387-404. *In*R. Lal (ed.) Soil processes and the carbon cycle. CRC Press, Boca Raton, FL.

Shaw, J.N., and P.L. Mask. 2003. Crop residue effects on electrical conductivity of Tennessee Valley soils. Commun. Soil Sci. Plant Anal.34:747-763.

Sherrod, L.A., G. Dunn, G.A. Peterson, and R.L. Kolberg. 2002. Inorganic carbon analysis by modified pressure-calcimeter method. Soil Sci. Soc. Am. J. 66:299-305.

Starr, G.C., R. Lal, R. Malone, D. Hotheem, L. Owens, and J. Kimble. 2000. Modeling soil carbon transported by water erosion processes. Land Degrad. Develop. 11: 83-91.

Suddeth, K.A., J.W. Hummel, and J.S. Birrell. 1997. Sensors for site-specific management. p. 183-210. *In* F.J. Pierce and E.J. Sadler (eds.) The state of site-specific management for agriculture. ASA Misc. Publ., ASA, CSSA, and SSSA, Madison, WI.

Sudduth, K.A., Drummond, S.T., Kitchen, N.R. 2001. Accuracy issues in electromagnetic induction sensing of soil electrical conductivity for precision agriculture. Computers and Electronics in Agriculture 31: 239-264.

Terra, J.A., J.N. Shaw, D.W. Reeves, R.L. Raper, E. van Santen, and P.L. Mask. 2004. Soil carbon relationships with terrain attributes, electrical conductivity, and a soil survey in a coastal plain landscape. Soil Sci. 169:819-831.

Thompson, J.A. and R.K. Kolka. 2005. Soil carbon storage estimation in a forested watershed using quantitative soil-landscape modeling. Soil Sci. Soc. Am. J. 69:1086–1093.

USDA Soil Conservation Service. 1980. Soil survey of Whitman county Washington.

USDA. 1993. Soil Survey Manual. Natural Resources Conservation Service. U.S. Government Printing Office, Washington, D.C. 189 pp.

USDA, 1978. Palouse Cooperative River Basin Study, Soil Conservation Service, Forest Service, and Economics, Statistics and Cooperative Service, U.S. Government Printing Office, Washington D.C. 182 pp.

VandenBygaart, A.J., X.M Yang, B.D. Kay, and J.D. Aspinall. 2002. Variability in carbon sequestration potential in no-till soil landscapes of southern Ontario. Soil Tillage Research 65:231-241.

Table 14.1. Soil series taxonomic classification, field area, and soil organic carbon in the 37-ha Washington State University Cook Agronomy farm.

Soil series	Taxonomic classification	Field area	SOC† (0-30 cm)	SOC (30-153 cm)	SOC (0-153 cm)
Soil survey		(%)	Mg ha^{-1}	Mg ha^{-1}	Mg ha^{-1}
Naff	Fine-silty, mixed, superactive, mesic Typic Argixerolls	15	49a (17)	61a (31)	111a (22)
Palouse	Fine-silty, mixed, superactive, mesic Pachic Ultic Haploxerolls	50	55b (17)	69a (32)	125b (22)
Thatuna	Fine-silty, mixed, superactive, mesic Oxyaquic Argixerolls	35	59c (18)	90b (41)	149c (29)
			GLM R^2 and CV (%)		
			9 (18)	15 (37)	15 (26)
Soil series	Taxonomic classification	Field area	SOC (0-30 cm)	SOC (30-153 cm)	SOC (0-153 cm)
Field survey		(%)	Mg ha^{-1}	Mg ha^{-1}	Mg ha^{-1}
Staley	Fine-silty, mixed, superactive, mesic Calcic Haploxerolls	9	49a (20)	48a (38)	97a (25)
Naff	Fine-silty, mixed, superactive, mesic Typic Argixerolls	16	54ab (19)	69bc (35)	122bc (26)
Palouse	Fine-silty, mixed, superactive, mesic Pachic Ultic Haploxerolls	42	55b (17)	77cd (38)	132c (26)
Thatuna	Fine-silty, mixed, superactive, mesic Oxyaquic Argixerolls	25	59c (17)	84d (39)	143d (27)
Latah	Fine, mixed, superactive, mesic Xeric Argialbolls	7	59bc (21)	80bcd (39)	139bcd (27)
Caldwell	Fine-silty, mixed, superactive, mesic Cumulic Haploxerolls	1	59ns (1)	103ns (2)	163ns (1)
ALL		100	56 (18)	75 (40)	131 (28)
			GLM R^2 and CV (%)		
			8 (18)	11 (38)	12 (26)

†SOC = Soil Organic Carbon means; mean separation ($p \leq 0.1$) using Tukey; and coefficient of variation (CV) in parentheses. GLM=general linear model

Table 14.2. Pearson Correlation Coefficients ($p \leq 0.05$) between soil organic carbon (SOC) and soil properties and relative crop yield for each soil series.

Soil map unit	SOC	RYld†	Athck	BtP/A	Btdpth	BkP/A	Bkdpth	BwP/A	Bwdpth	EP/A	Edpth	ECaS	ECaF
Staley	0-30 cm	NS‡	NS	ND	ND	ND	NS	NS	NS	ND	ND	NS	NS
	30-153 cm	0.87	0.51	ND	ND	ND	0.75	NS	0.55	ND	ND	NS	NS
	0-153 cm	0.82	NS	ND	ND	ND	0.85	NS	NS	ND	ND	NS	NS
Naff	0-30 cm	0.64	0.49	ND	NS	NS	ND	NS	0.65	NS	NS	-0.38	NS
	30-153 cm	NS	0.44	ND	NS	NS	ND	NS	NS	NS	NS	NS	NS
	0-153 cm	0.38	0.48	ND	NS	NS	ND	NS	0.51	NS	NS	NS	NS
Palouse	0-30 cm	0.43	0.38	NS	NS	NS	ND	NS	0.32	NS	NS	-0.31	NS
	30-153 cm	NS	0.58	NS	NS	NS	ND	NS	0.48	NS	NS	NS	NS
	0-153 cm	NS	0.59	NS	NS	NS	ND	NS	0.47	NS	NS	NS	NS
Thatuna	0-30 cm	0.35	0.37	NS	0.36	NS	ND	NS	NS	NS	NS	-0.36	-0.29
	30-153 cm	NS	0.38	-0.32	0.62	-0.28	ND	NS	NS	NS	0.75	-0.39	NS
	0-153 cm	0.28	0.42	-0.32	0.61	-0.28	ND	NS	NS	NS	0.69	-0.43	NS

†RYld=relative crop yield; Athck=A horizon thickness; BtP/A=Bt horizon presence or absence; Btdpth=depth to the top of the Bt horizon; BkP/A=Bk horizon presence or absence; Bkdpth=depth to the top of the Bk horizon; BwP/A=Bw horizon presence or absence; Bwdpth=depth to the top of the Bw horizon; EP/A=E horizon presence or absence; Edpth=depth to the top of the E horizon; ECaS=apparent electrical conductivity measured in the spring; ECaF=apparent electrical conductivity measured in the fall.

‡NS=not significant; ND=not determined.

Table 14.3. Stepwise regression parameter coefficients, partial R^2 and model R^2 for soil organic carbon and soil properties for each soil series.

	Staley†	Staley	Staley	Naff	Naff	Naff	Palouse	Palouse	Palouse	Thatuna	Thatuna	Thatuna
	0-30	30-153	0-153	0-30	30-153	0-153	0-30	30-153	0-153	0-30	30-153	0-153
Inter‡	NS	6.51	47.9	55.9	1.82	29.2	63.3	53.6	158.9	51.9	27.4	82.9
Athck				0.273	0.642	0.941	0.215	0.964	1.199	0.138		
				0.24	0.19	0.23	0.15	0.33	0.35	0.09		
BkP/A				-12.20								
				0.05								
Bkdpth		0.460	0.540									
		0.64	0.47									
Btdpth					0.283	0.550						
					0.08	0.07						
BwP/A									-47.63			
									0.02			
EP/A				7.98	13.23	20.93		-24.16	-37.80			
				0.14	0.07	0.10		0.04	0.03			
Edpth											0.953	1.021
											0.57	0.48
ECaSp				-0.559			-0.662	-2.127	-2.857			
				0.15			0.12	0.03	0.05			
ECaF								2.039	2.376			
								0.04	0.03			
Model R^2	0	0.64	0.47	0.58	0.34	0.40	0.27	0.44	0.49	0.09	0.57	0.48

† Soil series and depth increment in cm (0-30; 30-153 and 0-153); Regression parameter coefficients are listed at the top of the cell and partial regression R^2 are listed directly underneath the parameter coefficient.

‡Inter=intercept; Athck= A horizon thickness; BkP/A=Bk horizon presence or absence; Bkdpth=depth to the top of the Bk horizon;Btdpth=depth to the top of the Bt horizon; BwP/A=Bw horizon presence or absence; EP/A=E horizon presence or absence; Edpth=depth to the top of the E horizon; ECaS=apparent electrical conductivity measured in the spring; ECaF=apparent electrical conductivity measured in the fall.

Table 14.4. Pearson Correlation Coefficients ($p \leq 0.05$) between soil organic carbon (SOC) and terrain attributes for each soil series.

Soil map unit	SOC	Elev†	GloIrr	Slope	TRSP	CurTan	CurPln	CurPro	FlowD	FlowA	SCA	WetInd
Staley	0-30 cm	NS	NS	NS	NS	NS	NS	NS	0.57	NS	NS	NS
	30-153 cm	NS	-0.58	NS	-0.63	-0.64	-0.55	NS	0.65	NS	NS	ND
	0-153 cm	NS	-0.53	NS	-0.65	-0.54	NS	NS	0.72	NS	NS	ND
Naff	0-30 cm	NS	NS	-0.61	NS	NS	NS	NS	NS	NS	NS	NS
	30-153 cm	NS	NS	NS	NS	NS	NS	NS	NS	NS	NS	NS
	0-153 cm	NS	NS	NS	NS	NS	NS	NS	NS	NS	NS	NS
Palouse	0-30 cm	NS	NS	NS	NS	-0.31	-0.34	0.26	NS	0.25	0.25	0.35
	30-153 cm	NS	-0.23	0.34	NS	-0.50	-0.44	0.59	NS	0.29	0.29	0.30
	0-153 cm	NS	-0.25	0.28	NS	-0.50	-0.47	0.57	NS	0.31	0.31	0.35
Thatuna	0-30 cm	0.23	NS	0.37	NS	NS	NS	NS	NS	-0.32	-0.32	NS
	30-153 cm	NS	NS	0.38	NS	NS	NS	0.30	NS	NS	NS	NS
	0-153 cm	NS	NS	0.42	NS	NS	NS	NS	NS	NS	NS	NS

†Elev=elevation; GloIrr=global irradiation; Slope=slope; TRSP=TRASP; CurTan=tangential curvature; CurPln=plan curvature; CurPro=profile curvature; FlowD=flow direction; FlowA=flow accumulation; SCA=specific catchment area; WetInd=wetness index. NS=not significant

Table 14.5. Stepwise regression parameter coefficients, partial R^2 and model R^2 for soil organic carbon and terrain attributes for each soil series.

	Staley†	Staley	Staley	Naff	Naff	Naff	Palouse	Palouse	Palouse	Thatuna	Thatuna	Thatuna
	0-30	30-153	0-153	0-30	30-153	0-153	0-30	30-153	0-153	0-30	30-153	0-153
Inter‡	-767.5	189.2	88.69	315.2	NS	161.0	53.51	322.8	386.5	-415.6	90.07	154.1
Elev	1.025			-0.300						0.707		
	0.14			0.06						0.06		
GloIrr		-0.00008						-0.00017	-0.00017	0.00004		
		0.09						0.02	0.07	0.06		
Slope				-3.128		-5.641				-2.014	-1.871	-2.581
				0.37		0.12				0.07	0.03	0.04
TRASP							-4.451	48.92	47.70			
							0.03	0.04	0.02			
CurPln			56.67	-36.23							-32.54	-42.82
			0.08	0.06							0.06	0.08
CurPro								53.91	61.06	8.34	32.76	32.13
								0.35	0.32	0.04	0.09	0.07
CurTan		-347.6	-86.09	190.88			-72.64	-248.71	-327.6			
		0.24	0.13	0.05			0.03	0.03	0.05			
SCA										-0.00215		-0.00842
										0.10		0.06
FlowA											-0.057	
											0.03	
FlowD	0.220	0.168	0.533					0.185	0.224			
	0.33	0.42	0.52					0.02	0.02			
WetInd							0.906					
							0.12					
Model R^2	0.47	0.75	0.73	0.54	0	0.12	0.18	0.46	0.48	0.33	0.22	0.25

† Soil series and depth increment in cm (0-30; 30-153 and 0-153); Regression parameter coefficients are listed at the top of the cell and partial regression R^2 are listed directly underneath the parameter coefficient.

‡ Inter=intercept; Elev=elevation; GloIrr=global irradiation; Slope=slope; TRASP=TRASP; CurPln=plan curvature; CurPro=profile curvature; CurTan=tangential curvature; FlowA=flow accumulation; SCA=specific catchment area; FlowD=flow direction; WetInd=wetness index.

Table 14.6. Stepwise regression parameter coefficients, partial R^2 and model R^2 for soil organic carbon, terrain attributes and soil properties for each soil series.

	Staley†	Staley	Staley	Naff	Naff	Naff	Palouse	Palouse	Palouse	Thatuna	Thatuna	Thatuna
	0-30	30-153	0-153	0-30	30-153	0-153	0-30	30-153	0-153	0-30	30-153	0-153
Inter‡	-861.0	7.57	-1317.4	76.30	1.82	29.25	64.40	175.6	299.3	-332.0	26.93	151.3
Athck				0.162	0.638	0.941	0.184	0.731	0.967			
				0.11	0.19	0.23	0.15	0.18	0.35			
BkP/A				-15.00				28.39	53.34			
				0.07				0.02	0.04			
Bkdpth		0.390	0.323									
		0.64	0.27									
Btdpth					0.283	0.350						
					0.08	0.07						
BwP/A								-30.12	-33.50			
								0.01	0.01			
EP/A					13.23	20.93		-28.75	-25.32			
					0.07	0.10		0.03	0.02			
Edpth											0.915	0.804
											0.57	0.48
ECaS				-0.377			-0.631	-1.153		-0.483		-1.1096
				0.07			0.12	0.01		0.12		0.05
ECaF								2.073				
								0.02				
Elev	1.144		1.737							0.521		
	0.16		0.06							0.15		
GloIrr								-0.000065	-0.00011			
								0.08	0.09			
Slope				-2.515						-1.570		-3.363
				0.37						0.09		0.04
CurPln				-8.806			-9.972		-23.32			
				0.04			0.05		0.02			
CurPro									55.02		14.36	
									0.17		0.02	
CurTan								-186.7				-280.19
								0.01				0.04
FlowD	0.217	0.254	0.507									
	0.32	0.23	0.53									
WetInd										1.105		
										0.12		
Model R^2	0.48	0.87	0.86	0.66	0.34	0.40	0.32	0.72	0.69	0.48	0.59	0.61

†Soil series and depth increment in cm (0-30; 30-153 and 0-153); Regression parameter coefficients are listed at the top of the cell and partial regression R^2 are listed directly underneath the parameter coefficient.

‡ Inter=intercept; Athck= A horizon thickness; BkP/A=Bk horizon presence or absence; Bkdpth=depth to the top of the Bk horizon; Btdpth=depth to the top of the Bt horizon; BwP/A=Bw horizon presence or absence; EP/A=E horizon presence or absence; Edpth=depth to the top of the E horizon; ECaS=apparent electrical conductivity measured in the spring; ECaF=apparent electrical conductivity measured in the fall; Elev=elevation; GloIrr=global irradiation; Slope=slope; CurPln=plan curvature; CurPro=profile curvature; CurTan=tangential curvature; FlowD=flow direction; WetInd=wetness index.

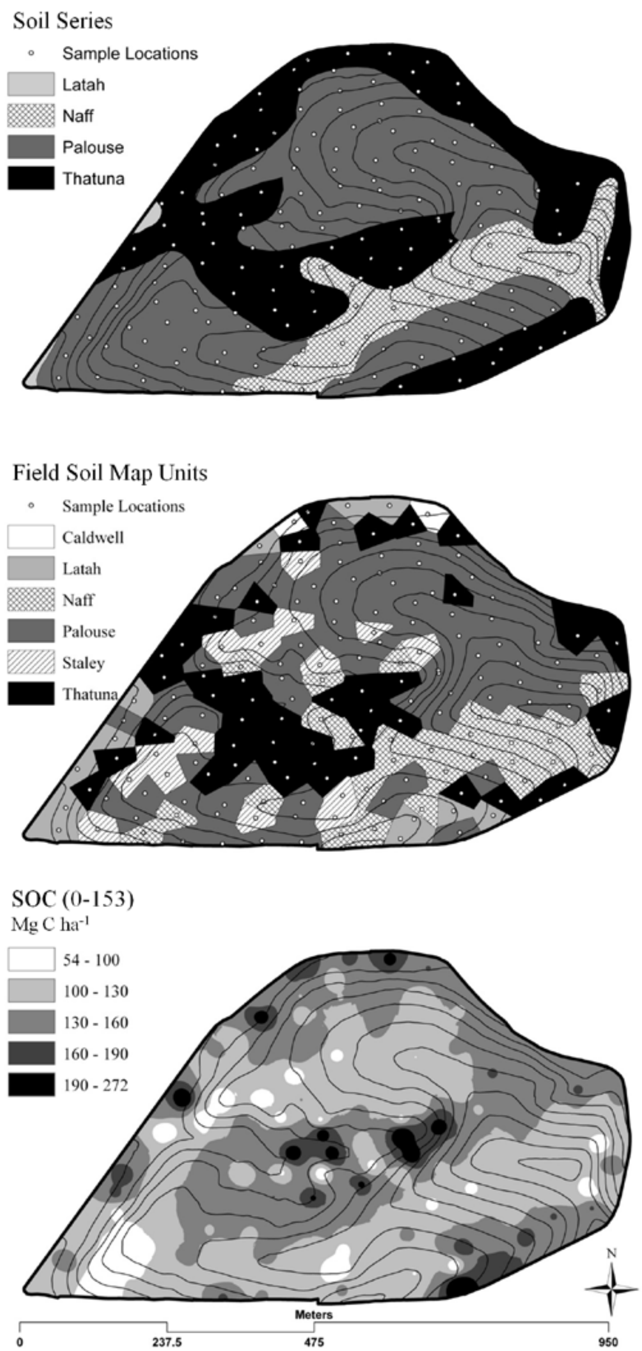

Figure 1

Figure 14.1. Maps of soil series, field soil map units and soil profile soil organic carbon (SOC, 0-153 cm) for the 37-ha Cook Agronomy Farm.

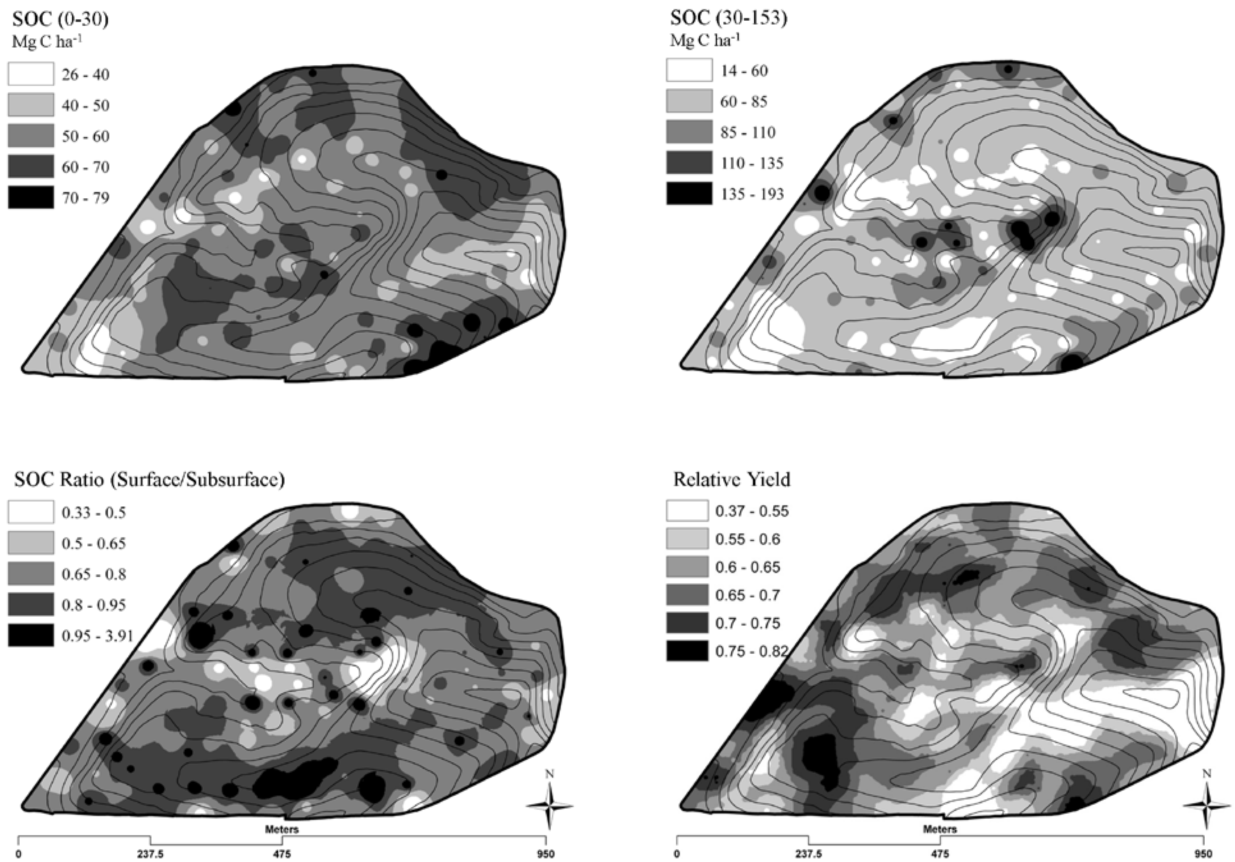

Figure 2

Figure 14.2. Surface soil organic carbon (SOC, 0-30 cm), subsurface soil organic carbon (SOC, 30-153 cm), the ratio of surface to subsurface soil organic carbon (SOC) and relative crop yield for the 37-ha Cook Agronomy farm.

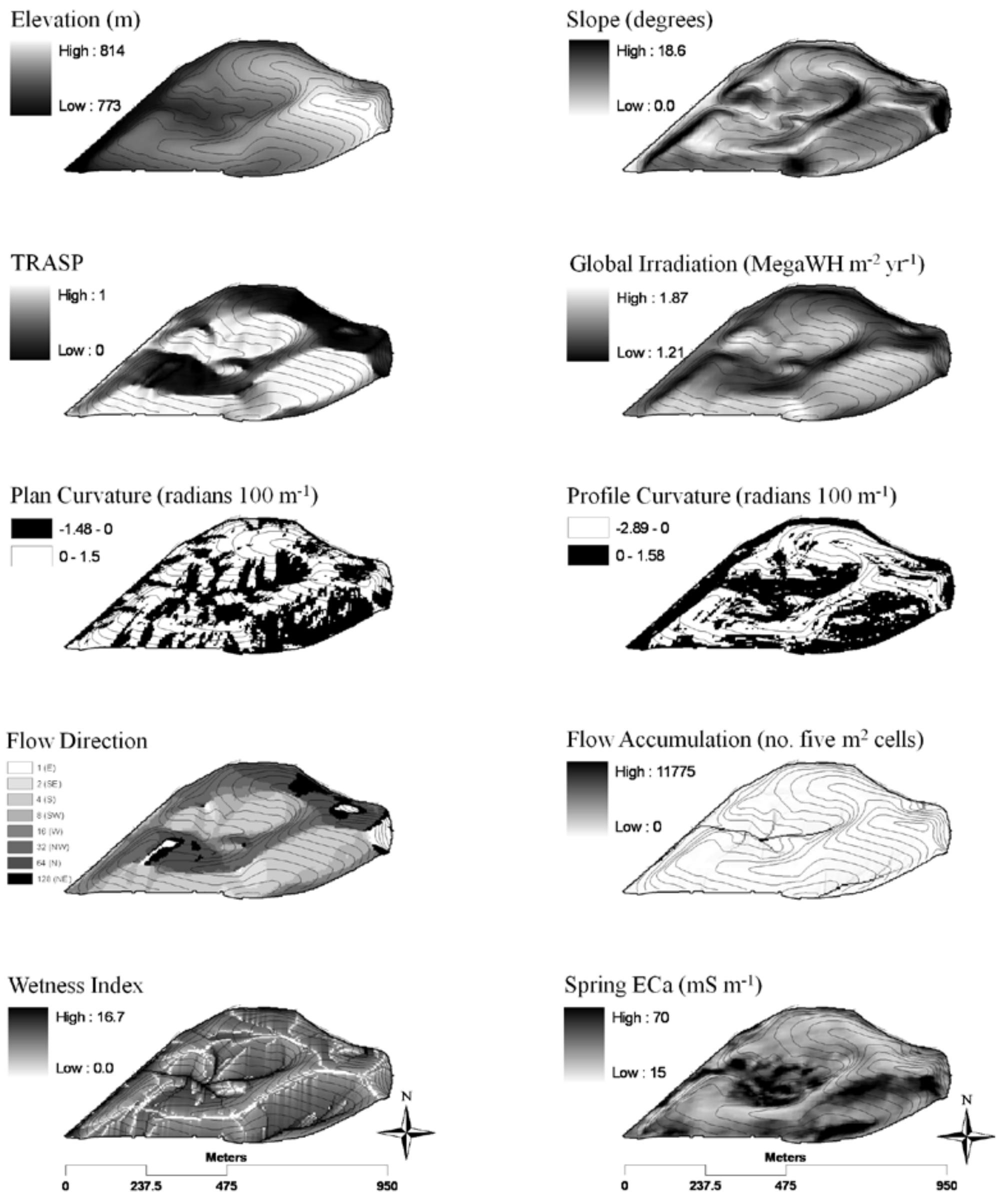

Figure 3

Figure 14.3. Terrain attributes and apparent electrical conductivity for the 37-ha Cook Agronomy Farm